Biomaterials 279 (2021) 121203

Contents lists available at ScienceDirect

Biomaterials

journal homepage: www.elsevier.com/locate/biomaterials

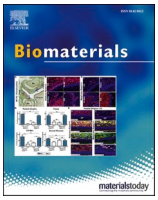

Control of osteoblast arrangement by osteocyte mechanoresponse through prostaglandin E2 signaling under oscillatory fluid flow stimuli

Tadaaki Matsuzaka [1], Aira Matsugaki [1], Takayoshi Nakano [*]

Division of Materials and Manufacturing Science, Graduate School of Engineering, Osaka University, 2-1 Yamada-oka, Suita, Osaka, 565-0871, Japan

ARTICLE INFO

Keywords:
Anisotropic collagen/apatite microstructure
mechanosensing
Osteocyte-osteoblast coculture
Cell orientation
PGE2

ABSTRACT

Anisotropic collagen/apatite microstructure is a prominent determinant of bone tissue functionalization; in particular, bone matrix modulates its anisotropic microstructure depending on the surrounding mechanical condition. Although mechanotransduction in bones is governed by osteocyte function, the precise mechanisms linking mechanical stimuli and anisotropic formation of collagen/apatite microstructure are poorly understood. Here we developed a novel anisotropic mechano-coculture system which enables the understanding of the biological mechanisms regulating the oriented bone matrix formation, which is constructed by aligned osteoblasts. The developed model provides bone-mimetic coculture platform that enables simultaneous control of mechanical condition and osteoblast-osteocyte communication with an anisotropic culture scaffold. The engineered coculture device helps in understanding the relationship between osteocyte mechanoresponses and osteoblast arrangement, which is a significant contributor to anisotropic organization of bone tissue. Our study showed that osteocyte responses to oscillatory flow stimuli regulated osteoblast arrangement through soluble molecular interactions. Importantly, we found that prostaglandin E2 is a novel determinant for oriented collagen/apatite organization of bone matrix, through controlling osteoblast arrangement.

1. Introduction

Bone is a complex, multicellular tissue that represents a characteristic microstructure controlled by the mechanical environment [1]. Its unique oriented architecture allows bone tissue functionalization depending on the surrounding stress distribution [2]. For example, ulnar tissue shows a highly aligned collagen/apatite bone matrix structure, which possesses mechanical properties that are stronger in the longitudinal direction than in the transverse direction [3]. There is increasing evidence that the microstructural arrangement of bone matrix is a dominant contributor to the functional adaptation of bone tissue to the mechanical environment [4]. Long-term bedridden or spaceflight environments severely weaken bones because of a decrease in loading levels [5,6]. Moreover, skeletal unloading induces a deteriorated microstructure of the bone matrix in relation to abnormal osteocyte arrangement [7]. Osteocytes play a central role in sensing mechanical stimuli and converting them into biochemical signals orchestrated with osteoblasts and osteoclasts [8]. In particular, osteocytes communicate with osteoblasts via soluble factors through the lacunar-canaliculi network inside the mineralized matrix [9–11]. Recent findings indicate that the anisotropic microstructure of bone tissue is strictly controlled by osteocyte function [12,13]. Besides the above role of osteocytes as a control tower of bone regulation, osteoblasts directly contribute to bone matrix orientation depending on the degree of their alignment [14,15]. It is important that the degree of bone tissue anisotropy can be estimated quantitatively from the osteoblast alignment in response to scaffold orientation [16]. Elucidation of osteoblast-osteocyte interaction scenarios governing the anisotropic morphological regulation under mechanical conditions can aid in the development of biomedical devices or a therapeutic target for the recovery of bone function.

Artificial control of mechanical stimuli to osteocytes has been previously investigated using *in vivo* loading models [17] and *in vitro* shear stress models [18,19]. Although these studies promoted the understanding of biological responses to mechanical conditions at tissue or molecular levels, the role of osteocytes in the regulation of anisotropic collagen/apatite construction of bone tissue, the strong modulator of mechanofunction in bone tissue, is not fully understood. Moreover, osteoblast-osteocyte coculture devices need to satisfy both mechanical

* Corresponding author. Division of Materials and Manufacturing Science, Graduate School of Engineering, Osaka University, Osaka, Japan.
E-mail address: nakano@mat.eng.osaka-u.ac.jp (T. Nakano).
[1] These authors contributed equally to this work.

https://doi.org/10.1016/j.biomaterials.2021.121203
Received 10 November 2020; Received in revised form 7 October 2021; Accepted 20 October 2021
Available online 21 October 2021

and architectural properties of bone tissues to mimic intercellular communications in the bone. Mechanical control of osteocyte function, in combination with biomaterials as a scaffold for osteoblast adherent substrates, may provide a powerful system that allows us to determine the molecular mechanisms underlying bone tissue functionalization. During physical activity, the bone matrix deforms, generating interstitial fluid flow through the canaliculi; osteocytes embedded in the bone matrix sense the applied mechanical stress as shear stress generated on the cell surface [20,21]. Under physiological conditions, bone tissue is exposed to dynamic mechanical conditions, which generate oscillatory flow stimuli to osteocytes. Here, we propose a novel coculture device for understanding the relationship between osteocyte mechanosensing and osteoblast alignment. The developed coculture model enables simultaneous regulation of osteocyte mechanical stimulation and osteoblast adhesion on an anisotropic culture scaffold. Osteocytes stimulated by the oscillatory flow, but not unidirectional steady flow, resulted in high level of osteoblast arrangements along the substrate collagen. Of note, prostaglandin E2 (PGE2), a stress-responsive molecule produced by osteocytes, was found to be a novel guiding cue that controls the anisotropic bone matrix arrangement through regulating the osteoblast alignment via PGE2-EP2/EP4 pathway.

2. Materials and methods

2.1. Fabrication of the oriented collagen substrates

Oriented collagen substrates were produced using a hydrodynamic extrusion method. Rat tail collagen type I was prepared at a concentration of 10 mg/mL in 0.02 N acetic acid. Collagen deposition into phosphate buffer saline (PBS, 10× concentration) was controlled by a three-axis robotic arm (SM300-3A; Musashi Engineering, Tokyo, Japan), which could regulate deposition speed and direction of collagen molecular fibrils; deposition speed of the robotic arm was set at 400 mm/s.

2.2. Isolation and culture of osteoblasts

Primary osteoblasts were isolated from calvariae of newborn mice by sequential enzymatic treatment. Calvariae were extracted from newborn C57BL/6 mice (3 days old) and placed in ice-cold α-MEM (Invitrogen, Carlsbad, CA). Fibrous tissues around the bone were cleanly removed, finely cut, and washed with Hank's balanced salt solution (Gibco). The extracted calvariae were then treated with collagenase/trypsin (collagenase: Wako, Osaka, Japan; trypsin: Nacalai Tesque, Kyoto, Japan) five times at 37 °C for 15 min each. The supernatants of the first two treatments were discarded, and the supernatants of the third, fourth, and fifth treatments were collected in α-MEM. Collections were passed through a 100-μm mesh strainer (BD Biosciences, San Jose, CA, USA), centrifuged, and the supernatant was removed. Extracted cells were resuspended in α-MEM containing 10% fetal bovine serum (FBS; Gibco), 1% penicillin, and streptomycin (Invitrogen, Carlsbad, CA) for cell culture. All animal experiments were approved by the Osaka University Committee for Animal Experimentation. Isolated osteoblasts were seeded onto each oriented collagen substrate at a density of 4,000 cells/cm^2, and were incubated at 37 °C in 5% CO_2.

2.3. Isolation and culture of IDG-SW3

IDG-SW3 cells (Applied Biological Materials, Canada) were cultured on rat tail type I collagen-coated plates (Thermo Fisher Scientific) under proliferative conditions at 33 °C in α-MEM containing 10% FBS, 1% penicillin and streptomycin, and interferon (IFN)-γ (Invitrogen). To induce differentiation, IDG-SW3 cells were seeded at a density of 80,000 cells/cm^2 with 50 μg/mL ascorbic acid and 4 mM β-glycerophosphate at 37 °C without IFN-γ. After 14 days of culture under differentiation conditions, cells were collected by treatment with trypsin, collagenase, and EDTA. Cells were analyzed and sorted using a fluorescent activated cell sorter equipped with a 488-nm laser (FACS, Aria IIIu cell sorter, BD Biosciences). Cell debris, dead, or doublet cells were excluded by selective gating of the area, width, and height of the scattered light plots. The resultant single cell population expressing the top 30% green fluorescent protein (GFP) intensity was collected as stress-responsive mature osteocytes. Data analysis was performed using the BD FACS Diva software (BD Biosciences). The sorted cells were seeded at a density of 80,000 cells/cm^2 under the differentiation conditions mentioned above, and were observed under a fluorescence microscope (BZ-X710, Keyence, Osaka, Japan). To verify the response to external stimuli and signaling through the intercellular network, the cells were treated with calcium indicator (Fluo 4-AM, DOJINDO, Kumamoto, Osaka) and then stimulated with a manipulation system (InjectMan, Eppendorf, Hamburg, Germany) equipped with microcapillary (Femtotips, Eppendorf).

2.4. Anisotropic coculture model with controlled fluid flow stimuli

A novel anisotropic coculture model of osteoblasts-osteocytes under controlled mechanical stimuli was constructed by designing a custom-made fluid flow stimuli system in combination with a horizontal coculture platform (Ginrei lab, Ishikawa, Japan). More importantly, osteoblast culture was conducted on the anisotropic culture scaffold, which provides a one-directional arrangement of collagen molecules. This system enables intercellular communication between osteoblasts and osteocytes through hydrophilic polycarbonate membranes with 0.6 μm pores (Ginrei lab) [22,23]. Fluid flow stimuli to osteocytes were controlled by designing and developing a cone-and-plate system composed of a rotating DURACON® cone with a 10° cone angle (Strex, Osaka, Japan). Osteoblasts were seeded at a density of 4,000 cells/cm^2 on the oriented collagen substrate on one side of the coculture device. The sorted IDG-SW3 cells were cultured at a density of 25,000 cells/cm^2 on the other side of the device, which was equipped with a rotating cone.

2.5. Particle imaging velocity (PIV)

The dynamics of fluid flow that stimulated osteocytes were analyzed using PIV. Tracer particles for PIV were determined considering the density and kinematic viscosity of the cell culture medium, according to the Baset-Boussinesq-Oseen equation as follows [24].

$$\frac{\pi d^3}{6}\cdot\rho_P\cdot\frac{du_P}{dt} = 3\pi\nu\rho_f d\left(u_f - u_p\right) + \frac{\pi d^3}{6}\cdot\rho_f\cdot\frac{du_f}{dt} + \frac{1}{2}\cdot\frac{\pi d^3}{6}\cdot\rho_f\left(\frac{du_f}{dt} - \frac{du_p}{dt}\right) + \frac{3}{2}\cdot d^2\rho_f\sqrt{\pi\nu}\int\frac{d\xi\left(\frac{du_f}{dt} - \frac{du_p}{dt}\right)}{\sqrt{t-\xi}},$$

where d is the tracer particle diameter and ν is the kinematic viscosity of the liquid. u_p, u_f, ρ_p, and ρ_f are the velocities and densities of the tracer particles and fluid, respectively. The first term on the right-hand side of the equation is the Stokes' drag force for instantaneous relative velocity. The second term is the Froude–Krylov force due to pressure gradient in undisturbed flow; the third term is the added mass force and the last

term is the Basset history integral. Glass hollow particles with a mean diameter of 10 μm were used to ensure the traceability of the particles. Colorless culture medium (600 μl), in which the particles were diffused, was placed in a well, and cone rotation was regulated under motor control. Particles 1 mm away from the plate surface were photographed at 1 ms intervals and recorded. Recorded images were used for calculating the fluid velocity using Davis 10.0 (LAVISION).

2.6. Cell viability assay

The Live/Dead Cell Staining Kit II (PromoKine) was used to quantify cell viability. After the fluid flow stimulations, cells were washed twice with PBS and incubated with calcein-AM and ethidium homodimer-3 (Dojindo) for 45 min at room temperature. Green fluorescent and red fluorescent cells were counted as live and dead cells, respectively, under a fluorescence microscope (BZ-X710, Keyence, Osaka, Japan). The ratios of live/dead cells were calculated.

2.7. Immunofluorescence staining

Osteoblasts on the oriented collagen substrates cocultured with osteocytes were fixed with 4% formaldehyde in PBS at room temperature for 20 min, and were then washed with PBST (PBS-0.05% Triton X-100). PBST containing 5% normal goat serum (Invitrogen) was used to block non-specific binding sites at room temperature for 30 min. For immunostaining of vinculins, cells were incubated with mouse monoclonal antibodies against vinculin (Sigma-Aldrich) at 4 °C overnight. After rising with PBS, cells were exposed to secondary antibodies (Alexa Fluor 546-conjugated anti-mouse IgG, Invitrogen) and DAPI (Invitrogen), and were further incubated at room temperature for 2 h. For visualization of F-actin, cells were exposed to Alexa Fluor 488-conjugated phalloidin (Invitrogen). Finally, cells were washed with PBST, mounted with Prolong Diamond Antifade Reagent (Invitrogen), and observed under a fluorescence microscope (BZ-X710, Keyence, Osaka, Japan).

2.8. Analysis of cell orientation

The degree of cell orientation with respect to the collagen running orientation of substrates was evaluated by taking photographs of fluorescent cells obtained via a fluorescence microscope (BZ-X710, Keyence, Osaka, Japan). Cell orientation was quantitatively analyzed using the Cell Profiler software (Broad Institute, Cambridge, MA), and degree of cell arrangement, R, was calculated using the following equation.

$$R = 2\left(\cos^2\theta - \frac{1}{2}\right) \tag{1}$$

$$\cos^2\theta = \left(\sum_{1}^{n}\cos^2\theta\right)\Big/ n \tag{2}$$

2.9. Gene expression analysis

Total RNA was isolated from osteocytes or osteoblasts using TRIzol reagent (Invitrogen) according to manufacturer's instructions. Gene expression levels were assessed using quantitative real-time PCR (Stepone, Applied Biosystems, CA, USA). In PCR analysis, the threshold cycle (Ct) value was set within the exponential phase of the PCR reaction, and the ΔCt value for each target gene was determined by subtracting the Ct value obtained for GAPDH (internal control) from the target gene. Results were normalized using expression levels determined in control cells.

For comparison of gene expression under different mechanical stimulation conditions, total RNA was extracted using NucleoSpin RNA Plus XS (MACHEREY-NAGEL). Gene expression profiles were obtained using a NovaSeq 6000 system (Illumina, San Diego, CA, USA) according to manufacturer's guidelines. Briefly, RNA purity and integrity were evaluated using electrophoresis via the Agilent 2200 TapeStation (Agilent Technologies, Santa Clara, CA, USA). Two indexed libraries were pooled and sequenced. After that, data analysis was performed using the Genedata Profiler Genome software (Genedata). RNA seqence data was imported into integrated differential expression and pathway analysis (iDEP v.0.93), an integrated application software for gene ontology analysis. The target genes expressing the intensity more than 1.5-fold in the oscillatory flow condition compared to those in the control were indicated as a normalized value by a color bar.

2.10. Blocking of EP2 and EP4 receptor

The effects of PGE2 on osteoblast arrangement were investigated using a PGE2 antagonist. PGE2 receptor EP2- and EP4- specific inhibitors, TG6-10-1 (Merck) and L-161982 (Sigma-Aldrich), were used to stimulate primary osteoblasts 24 h after seeding, at a final concentration of 10^{-6} M for 48 h [25,26]. The osteoblasts were immunostained and the degree of cell orientation was analyzed as described in section 2.8.

2.11. Statistical analysis

Values are reported as mean ± standard deviation. Statistical significance between two groups was tested using the Student's t-test or the Welch's *t*-test. For comparison among three groups, one-way analysis of variance was conducted, followed by Tukey's multiple comparison tests. Significance was established when $p < 0.05$, and $p < 0.01$.

3. Results

3.1. Isolation of mature osteocytes

DMP1-GFP is a marker of osteocyte differentiation. Fluorescence microscopy images of DMP1-GFP expression revealed that IDG-SW3 cells were successfully differentiated into GFP-positive osteocytes and isolated via cell sorting (Fig. 1A). When cultured under proliferative conditions, IDG-SW3 cells were GFP-negative. In contrast, IDG-SW3 cells cultured for 14 days under differentiation conditions showed GFP expression according to cell maturity, and adopted dendritic cell morphology. Mature osteocytes with GFP intensity in the top 30% were isolated and extracted from the 14-day IDG-SW3 cell culture and were sorted based on GFP levels (Fig. 1B). Gene expression analysis demonstrated that total GFP level was increased, thus confirming that mature osteocytes were accurately isolated (Fig. 1C). Moreover, the osteocytes responded to the mechanical stimulation, cell to cell spread of calcium signaling was observed among the cultured osteocytes (Fig. 1D).

3.2. Anisotropic coculture model with controlled mechanical stimuli

An anisotropic coculture system that mimics the bone microenvironment with stress fields was established (Fig. 2A). Isolated mature osteocytes and cocultured osteoblasts were separated by inserts, and only osteocytes were stimulated by fluid flow. PIV measurement demonstrated that osteocytes were stimulated by fluid flow that was precisely controlled by cone rotations (Fig. 2B). Cell morphology and viability were assessed by live/dead cell staining (Fig. 2C). Fluorescence microscope images of osteocytes located equidistant from the center of the well showed that cell shape was not significantly affected by flow stimulations. Unstimulated cells were 97.9 ± 0.8% viable; cells stimulated by fluid flow also retained good viability. Cells stimulated by steady flow and oscillatory flow were 97.0 ± 0.7% and 95.8 ± 2.1% viable, respectively (Fig. 2D).

3.3. Oscillatory flow stimulation to osteocytes regulate cocultured osteoblast arrangement through soluble factors

Osteoblasts were preferentially aligned along the substrate collagen

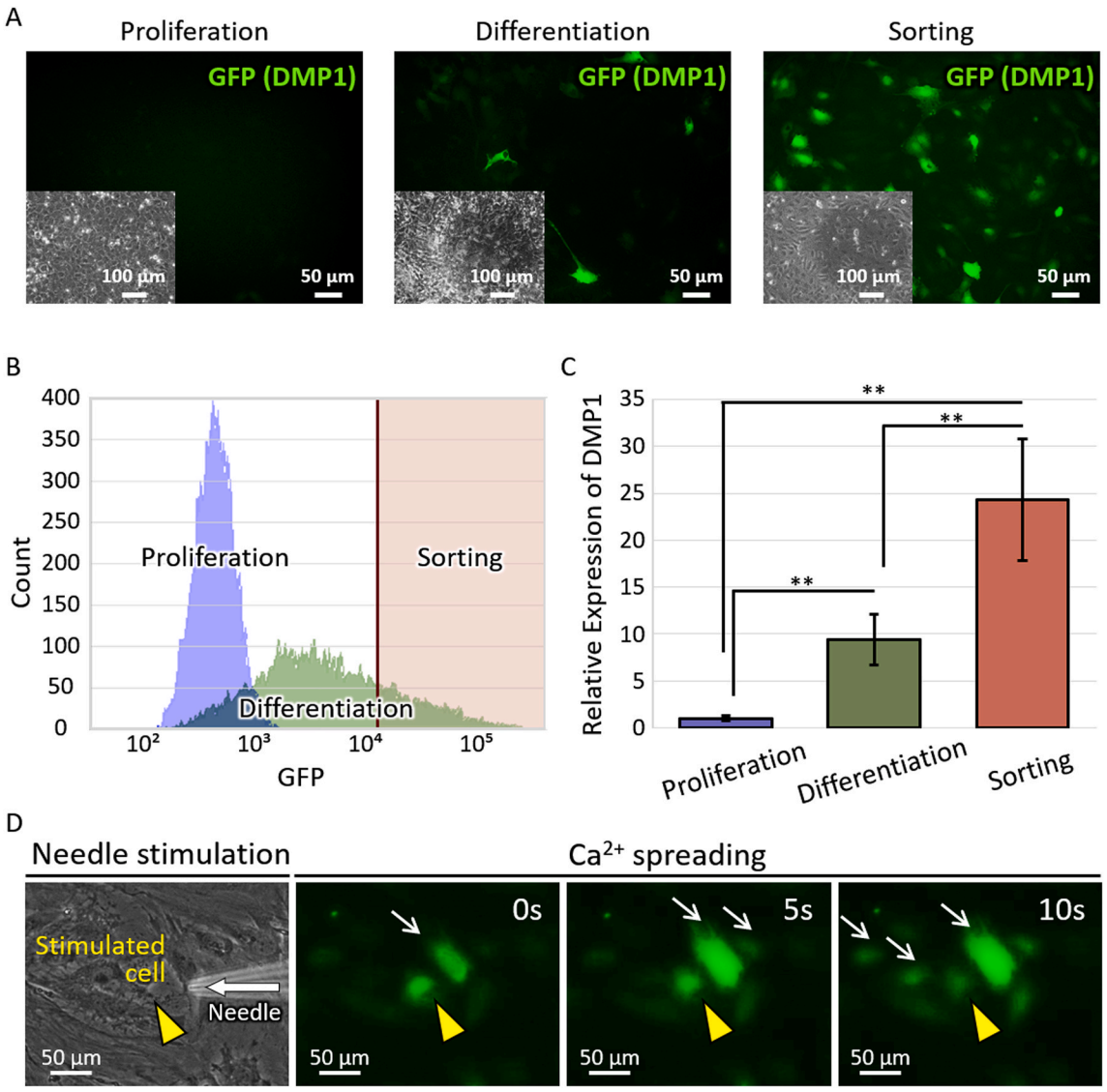

Fig. 1. Isolation of mature osteocytes from IDG-SW3 cells using cell sorting. (A) DMP1-GFP expression in IDG-SW3 at each differentiation stage. The insets show the phase-contrast images of the corresponding fluorescent images. (B) Histogram of GFP intensity for proliferation and differentiation induction. (C) Gene expression of DMP1 in IDG-SW3 at each differentiation stage. (D) Stimulation of a single osteocyte with a needle manipulator. Intercellular Ca^{2+} signaling was observed among the obtained osteocytes.

orientation. The degree of cell arrangement was comparable between the control and osteoblasts cocultured with osteocytes stimulated by steady flow. In contrast, osteoblasts cocultured with osteocytes stimulated by oscillatory flow showed significantly higher degree of orientation than the control or cells stimulated by steady flow (Fig. 3A and B). To determine which signaling pathways determined the osteoblast arrangement, comprehensive gene expression profiles of osteoblasts were obtained. The expression levels of *Myosin* family members (*Myl1*, *Myl4*, *Myl12a*, *Myo1d*, *Myo5a*, *Myo5c*, *Myof*), *Actin* family molecules (*Actn1*, *Actn4*), focal adhesion-related molecules (*Src*, *Cfl1*, *Pxn*), and *Integrin* family (*Itga5*, *Itgb1*, *Itgav*, *Itgb3*) were increased specifically in osteoblasts cocultured with oscillatory flow-stimulated osteocytes (Fig. 3C). These results indicated that osteocytes stimulated by oscillatory flow regulated the osteoblast cytoskeletal-adhesion construction via soluble factors, resulting in the high degree of cell alignment. To reveal the soluble factors responsible for osteoblast arrangement, alterations in gene expression in osteocytes in response to fluid flow stimuli were analyzed. No significant differences in *BMP2*, *Wnt5a*, *Sfrp1*, and *Sost* expression were found among control, steady, and oscillatory flow-stimulated osteocytes. Contrarily, oscillatory flow stimulation enhanced *Ptgs2* (encoding PGE2) expression as compared with those in control cells and those stimulated by steady flow (Fig. 3D).

3.4. The effects of PGE2 blockade on osteoblast arrangement

These results suggested that PGE2 secretion by osteocytes regulates osteoblast arrangement. To confirm that this effect is mediated by PGE2 activation, the PGE2 receptors on osteoblasts, EP2 and EP4, were blocked by antagonists. Osteoblast arrangement was disturbed by the addition of EP2 and EP4 receptor antagonists, indicating that PGE2-EP2/EP4 signaling is involved in osteocyte-mediated osteoblast arrangement (Fig. 4A and B). In addition, a significant reduction in focal adhesion molecules, *FAK* and *Pxn* was observed after the antagonist treatment, as well as the downregulation of the Integrin family including *Itga5*, *Itgav* and *Itgb3*.

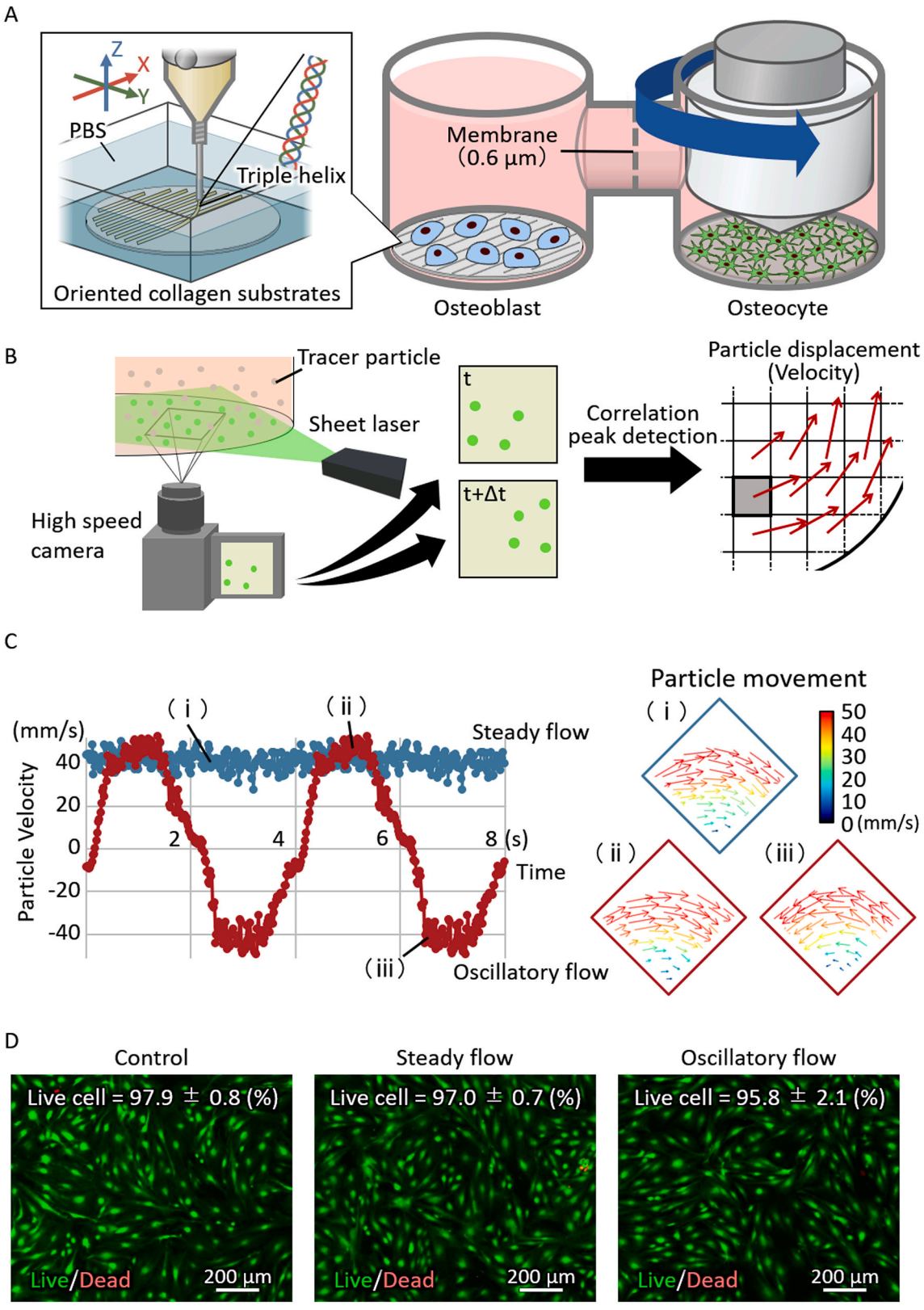

Fig. 2. Development of a novel coculture platform of fluid-flow-stimulated osteocytes and osteoblasts on oriented collagen substrate. (A) (Left) Schematic illustration of how oriented collagen substrates for osteoblasts were produced. (Right) Schematic illustration of the novel horizontal osteocyte-osteoblast coculture model. (B) Schematic illustration of fluid flow analysis by PIV; tracer particles were mixed into the flow field and a sheet laser beam was irradiated at 1 min time interval (Δt). Particles were photographed using a high speed camera, and the velocity of the particles was calculated from the cross-correlation peaks of the two corresponding images. (C) Results of the fluid flow analysis by PIV, as shown by the color plot, at average flow velocity with steady flow and oscillatory flow. (D) Results of the live/dead cell staining; live and dead cells are indicated by green and red fluorescence, respectively. (For interpretation of the references to color in this figure legend, the reader is referred to the Web version of this article.)

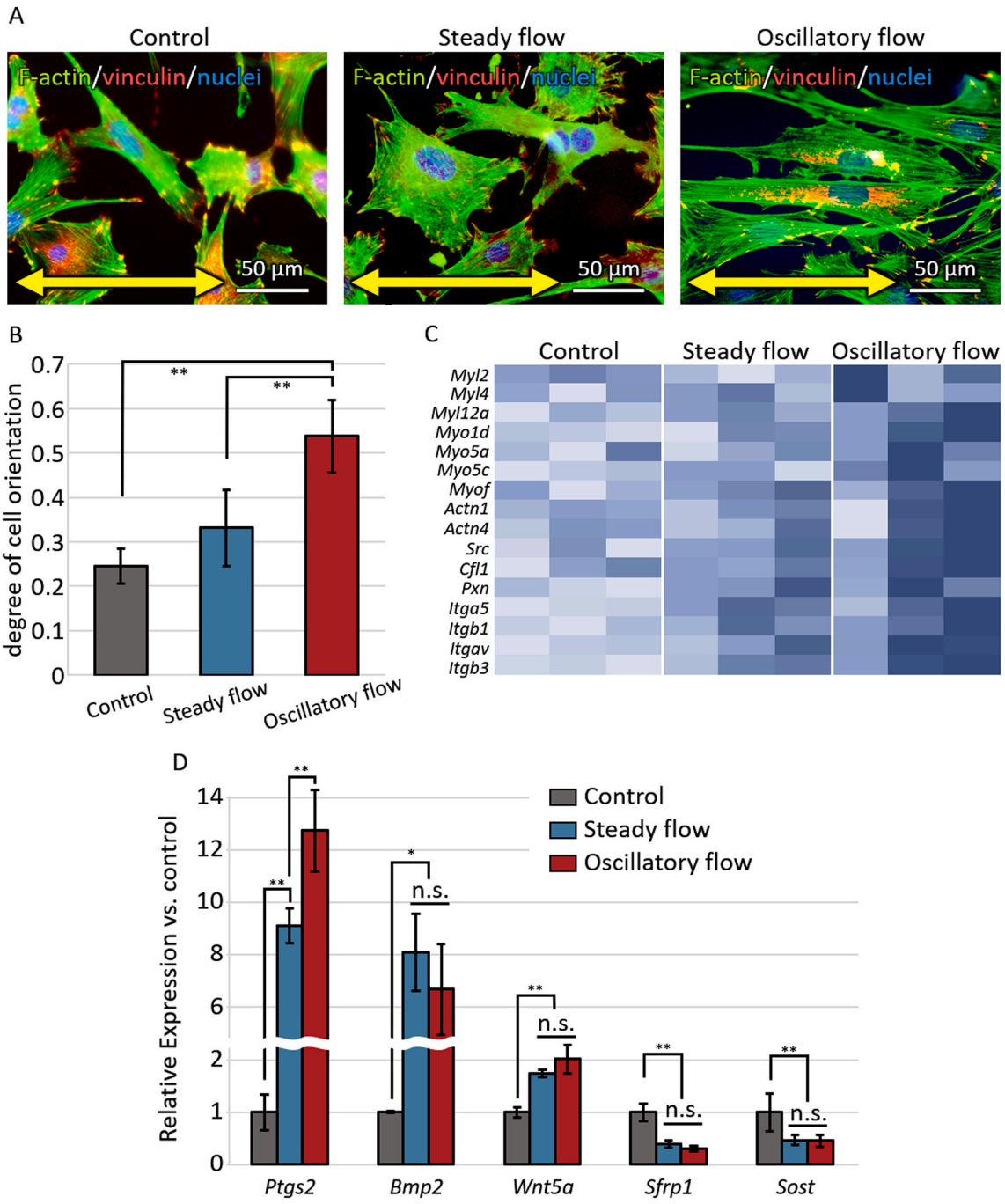

Fig. 3. Osteoblasts arrangement in response to control (no flow), steady flow or oscillatory flow. (A) Immunofluorescence images of osteoblast cultured on oriented collagen substrates with osteocyte loaded shear stress. (B) Comparison of the degree of cell orientation. **: $p < 0.01$ vs. control. (C) Comprehensive gene expression analysis in osteoblasts cocultured with fluid flow-stimulated osteocytes. (D) Comparison of osteocyte mechanosensing-related gene expression in response to steady and oscillatory flow. A significant difference in PGE2 gene expression is found between steady flow and oscillatory flow conditions.

4. Discussion

4.1. Construction of a novel coculture device of osteoblast-osteocyte with controlled fluid flow stimuli

In this study, we established a novel coculture platform in which osteoblasts and osteocytes can interact via soluble factors under fluid flow stimuli. Osteocyte functions have been previously studied using primary cells [27,28] or other cell lines [29,30]; however, these systems were insufficient for understanding the mechanical responses of osteocytes. In this study, the IDG-SW3 cell line, which express a series of differentiation markers, including those of osteoblasts and early and late osteocytes, was used [31]. Considering the effects of cellular heterogeneity depending on their differentiation stages, mature osteocytes that expressed fluorescence intensities above 30% of DMP1-GFP cells were isolated using cell sorting (Fig. 1A and B). The expression level of DMP1 in isolated cells was significantly higher as compared with that in the heterogeneous cell population during both proliferative and differentiation stages (Fig. 1C), indicating that fully maturated osteocytes were isolated with high accuracy. In addition, the intercellular calcium signaling in response to the mechanical stimulation was clearly observed in our coculture system (Fig. 1D). Considering osteocytes function

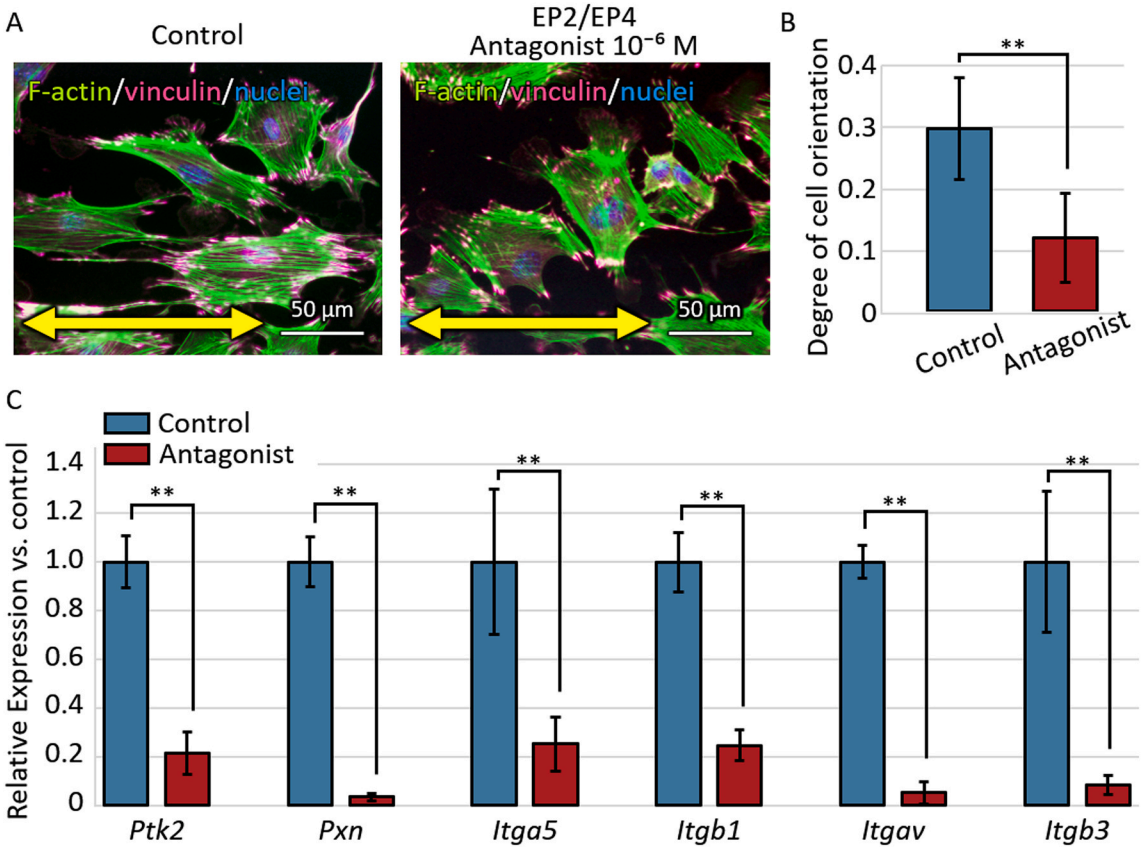

Fig. 4. The effects of PGE2 signaling on osteoblasts arrangement. (A) Immunofluorescence images of osteoblast treated with EP2/EP4 antagonist on oriented collagen substrates. Green, F-actin; red, vinculin; blue, nuclei. (B) Comparison of the degree of cell orientation. (C) Comparison of gene expression in osteoblasts treated with EP2/EP4 receptor antagonists. Focal adhesion molecules are enriched in control cells compared with EP2/EP4 blocked osteoblasts **: $p < 0.01$ vs. control. (For interpretation of the references to color in this figure legend, the reader is referred to the Web version of this article.)

depends on the surrounding environment, the 2D cultivation in this coculture system can further extend to 3D cultivation which mimics fully functional osteocytes [32,33].

The osteocyte and osteoblast coculture was classically investigated mainly using a transwell system, in which the cells are separated into upper and lower parts [34,35]. In addition, recent works developed some innovative methodology including 3D microfluidic coculture chips [32]. The present coculture platform provided an independent harvest environment, an anisotropic scaffold for osteoblast cultivation, and mechanical stimuli for osteocytes. The anisotropic collagen substrate was fabricated using extrusion method, whereas there have been reported various methodology to create oriented substrate including flow stimulation [36]. The horizontal connection between different cell types enabled simultaneous observation of both cells. Furthermore, our coculture system can be extended to human cell research. The human osteoblast alignment can also be evaluated by observing the response of cytoskeleton and focal adhesion activation in response to oriented collagen scaffold [37]. In summary, the present coculture system allowed us to understand the interaction between osteocytic responses against mechanical stimuli and osteoblastic alignment against substrates collagen orientation (Fig. 2A).

It is important that the fluid flow stimuli to the osteocytes in the present system were quantitatively controlled to simulate the flow condition inside the living bone considering the flow velocity and the size of the lacunar/canaliculi [38,39]. The flow stimuli were accurately loaded based on the PIV analysis (Fig. 2B and C). PIV analysis revealed that the applied shear stress well reflected the solute transport inside the lacunar-canaliculi system in bones with a maximum controlled fluid velocity of 40 mm/s. It also demonstrated that fluid flow stimuli were applied only to the osteocytes and no effects of stimulation in the separated wells for osteoblasts were noted. Live/dead staining revealed that both steady and oscillatory flow exhibited no statistically significant effects on cell viability when compared to the control group (Fig. 2D).

4.2. Osteocyte mechanosensing regulates osteoblast arrangement

Osteoblast orientation is one of the strong determinants of oriented bone matrix microstructure [14–16,40]. The degree of osteoblast alignment mirrors the level of bone matrix arrangement, which dominates the mechanical function of bone tissue [4]. In this study, osteoblast orientation was clearly affected by the different external mechanical conditions surrounding osteocytes, suggesting that different responses of osteocytes to mechanical conditions regulated the degree of osteoblast arrangement via soluble factors (Fig. 3A and B). Interestingly, it was first shown that the arrangement of osteoblasts was significantly influenced by oscillatory flow, but not by steady flow stimulation of osteocytes. In actual living systems, movement involves repeated loading and unloading conditions of the bone. The direction of fluid flow inside a lacunar/canaliculi network is reversed according to the loading/unloading condition [20]; oscillatory flow can work as a more physiologic flow than unidirectional flow [41]. The responses of osteocytes to different types of fluid shear stress, including constant, pulsatile, and oscillatory fluid flows, have been studied separately. The load magnitude, frequency, and number of cycles are considered possible factors that determine cellular responses [42–44]. However, the systematic understanding of the cellular responses to shear stress conditions of static or dynamic stimuli is currently lacking. In this study, we constructed a novel coculture device under controlled fluid flow stimuli,

which enabled the comparison between steady and oscillatory flow and its effects on osteocyte function. Furthermore, it is important that mechanically stimulated osteocytes can communicate with osteoblasts cultured on oriented collagen substrates, which mimics the bone matrix microstructure, via soluble proteins. The results indicate that osteoblast alignment is regulated by activated osteocytes in response to a relatively high frequency (0.25 Hz) oscillatory flow. Moreover, steady and oscillatory flow possibly affected osteocytes through different molecular pathways [45]. Although the exact mechanisms by which physical signals, such as mechanical loads, are converted into biochemical signals are not completely understood, a variety of cell surface proteins and structures, including integrins, primary cilia, and ion channels, have been proposed to function as a sensor of fluid stimulation in osteocytes [46–49]. These findings led us to consider the molecular interaction between osteoblasts and osteocyte mechanosensing in the regulation of osteoblast arrangement, which determine the functionalization of bone tissue based on anisotropic microstructural construction.

4.3. PGE2 mediates osteocyte stress response and osteoblast arrangement

In osteoblasts cocultured with oscillatory flow-stimulated osteocytes, which have the highest degree of cell orientation, the expression levels of *Myosin* family, cell adhesion-related proteins and *Integrin* family genes were increased. It is suggested that osteocyte stimulus induced the osteoblast actin/myosin-responsive focal adhesion construction involved in cytoskeletal deformation, resulting in the significant change in osteoblast orientation via intercellular indirect signal transmission (Fig. 3C). Several key genes associated with osteocyte mechanosensing were compared under control (no flow), steady, and oscillatory flow conditions. The expression level of all the examined genes was significantly altered in the presence or absence of mechanical stimuli (Fig. 3D); this finding is consistent with previous reports [50–52]. Among them, significant difference in PGE2 gene expression was found between steady flow and oscillatory flow conditions, which suggested that PGE2 secretion in response to steady or oscillatory flow can regulate osteoblast arrangement via intercellular signaling. Considering that steady flow does not seem to impact osteoblast arrangement, it was suggested that PGE2 expression likely promoted osteoblast arrangement in a concentration-dependent manner.

PGE2, an early response molecule to mechanical loading [53–55], acts on a variety of cells by activating four types of membrane receptors, EP1–EP4, which have different signal transduction properties [56,57]. Osteoblasts express EP2 and EP4 receptors, which have been recognized as a regulatory pathway involved in bone formation [58,59]. Although these previous findings suggested the role of PGE2 in bone metabolism in response to mechanical stimuli, its essential roles in bone functionalization has never been elucidated. In this study, osteoblasts treated with EP2 and EP4 receptor-specific antagonists induced loss of osteoblast arrangement on oriented collagen substrates (Fig. 4A and B). The findings revealed the novel role of PGE2/EP-EP4 signaling as an

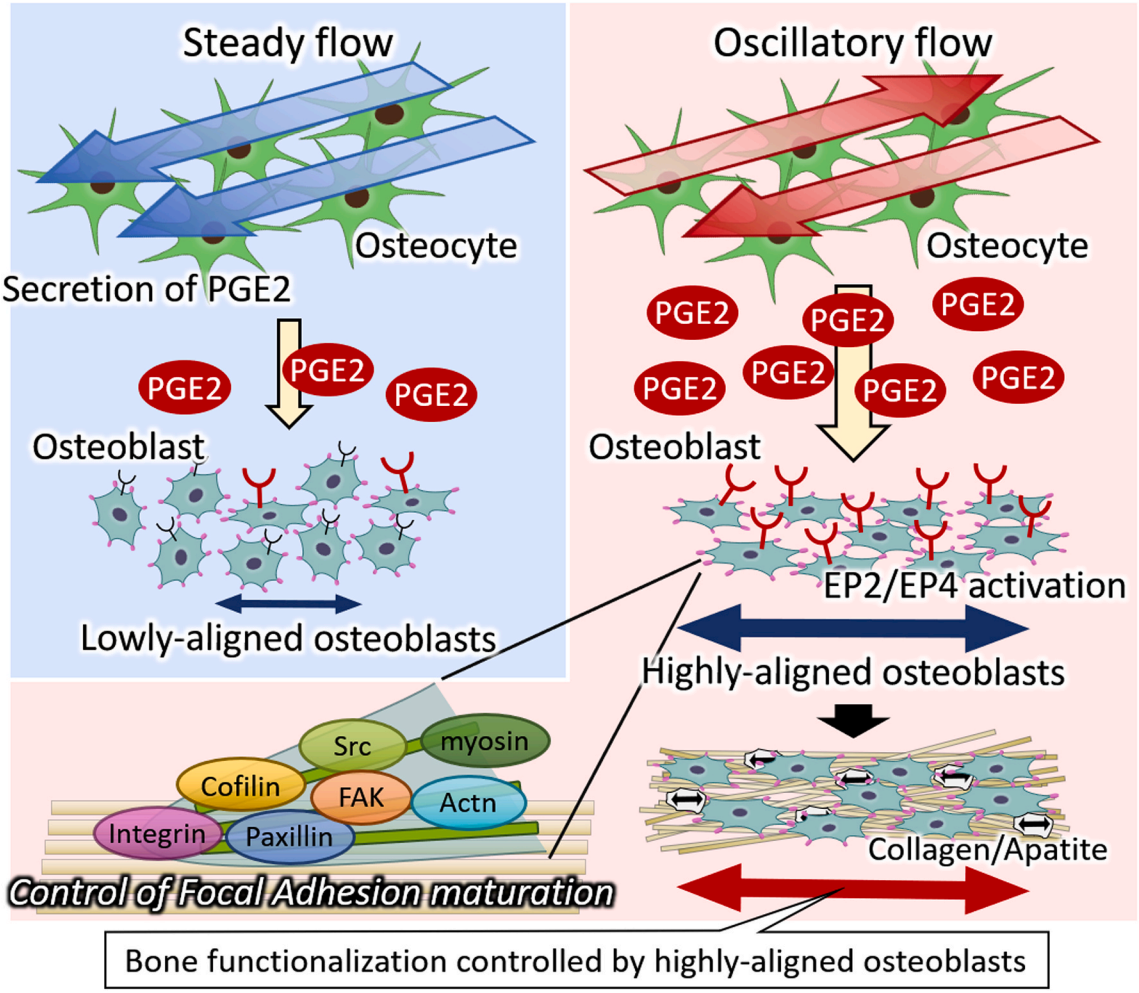

Fig. 5. Osteocyte responses to oscillatory flow stimuli promoted osteoblast arrangement via soluble mediator proteins. Notably, a novel role of PGE2 as a mediator for controlling osteoblast arrangement in response to oscillatory flow to osteocytes was found for the first time. The findings indicate PGE2 as an important target molecule to determine the anisotropic collagen/apatite bone matrix.

essential contributor for regulating osteoblast arrangement, which is one of the most important determinant in anisotropic bone matrix microstructure. Indeed, PGE2 signaling has been reported to be involved in cytoskeletal arrangement via the PKA signaling pathway [60]. Furthermore, PGE2 plays an important role in directional regulation of hair follicle morphogenesis [61]. It is interesting that the focal adhesion molecules were enriched in control cells compared with EP2/EP4 blocked osteoblasts (Fig. 4C). Previous study has shown that PGE2 is related to the cytoskeletal organization in osteoblasts [62]. Intact osteoblasts sense the molecular orientation of collagen that substrates via a specific amino acid sequence [63], which induces cytoskeletal arrangement along the running direction of the collagen fiber [64]. Upregulated PGE2 secretion from osteocytes in response to oscillatory fluid flow could stimulate downstream signaling in osteoblasts, resulting in greater cell alignment, and leading to bone tissue functionalization with highly aligned bone matrix construction (Fig. 5).

5. Conclusion

Bone tissue functionalization is governed by the oriented microstructure, which is modulated by multiple types of cells in response to the mechanical environment. Little is known, however, about the precise molecular mechanisms linking mechanical conditions and bone tissue organization. Simultaneous control of mechanical conditions and intercellular communication can provide a powerful platform to understand the cellular mechanisms in response to external stimuli. Here, we designed and developed a novel osteocyte-osteoblast communication system equipped with controlled shear stress stimulation and an anisotropic scaffold. Osteocyte responses to oscillatory flow stimuli promoted osteoblast arrangement via soluble mediator proteins. The developed anisotropic mechano-coculture system heralds the next-generation microstructural medicine in bone therapeutics, which have never been achieved so far. Notably, a novel role of PGE2 as a mediator for controlling osteoblast arrangement, a key regulator in bone functionalization was found for the first time. The findings can open up new avenues for the healing strategy of bone microstructure, overcoming the limitation of conventional bone mass regulation.

Credit author statement

Tadaaki Matsuzaka: Methodology, Formal analysis, Investigation, Writing - Original Draft, Visualization. **Aira Matsugaki**: Methodology, Formal analysis, Investigation, Writing - Original Draft, Validation, Visualization. **Takayoshi Nakano:** Conceptualization, Methodology, Validation, Writing – Review and Editing, Supervision, Project administration.

Data availability

The raw and processed data required to reproduce these findings are available for download from https://doi.org/10.17632/kwbxbkyvvk.1.

Declaration of competing interest

The authors declare that they have no known competing financial interests or personal relationships that could have appeared to influence the work reported in this paper.

Acknowledgments

This work was supported by Grants-in-Aid for Scientific Research (grant numbers 18H05254, 20H00308) from the Japan Society for Promotion of Science. The funders had no role in experiment planning, data collection and analysis, or decision to publish.

We thank Ms. Tanaka Y., Mr. Ueyama K., and Mr. Sakiyama K. of Japan Kanomax Co., Ltd for their helpful support in PIV analysis.

References

[1] P.J. Ehrlich, L.E. Lanyon, Mechanical strain and bone cell function: a review, Osteoporos. Int. 13 (2002) 688–700.
[2] T. Nakano, K. Kaibara, T. Ishimoto, Y. Tabata, Y. Umakoshi, Biological apatite (BAp) crystallographic orientation and texture as a new index for assessing the microstructure and function of bone regenerated by tissue engineering, Bone 51 (2012) 741–747.
[3] T. Nakano, K. Kaibara, Y. Tabata, N. Nagata, S. Enomoto, E. Marukawa, Y. Umakoshi, Unique alignment and texture of biological apatite crystallites in typical calcified tissues analyzed by microbeam X-ray diffractometer system, Bone 31 (2002) 479–487.
[4] T. Ishimoto, T. Nakano, Y. Umakoshi, M. Yamamoto, Y. Tabata, Degree of biological apatite c-axis orientation rather than bone mineral density controls mechanical function in bone regenerated using recombinant bone morphogenetic protein-2, J. Bone Miner. Res. 28 (2013) 1170–1179.
[5] T. Lang, A. LeBlanc, H. Evans, Y. Lu, H. Genant, A. Yu, Cortical and trabecular bone mineral loss from the spine and hip in long-duration spaceflight, J. Bone Miner. Res. 19 (2004) 1006–1012.
[6] J. Yang, J. Li, X. Cui, W. Li, Y. Xue, P. Shang, H. Zhang, Blocking glucocorticoid signaling in osteoblasts and osteocytes prevents mechanical unloading-induced cortical bone loss, Bone 130 (2020) 115108.
[7] J. Wang, T. Ishimoto, T. Nakano, Unloading-induced degradation of the anisotropic arrangement of collagen/apatite in rat femurs, Calcif. Tissue Int. 100 (2017) 87–94.
[8] A.G. Robling, L.F. Bonewald, The osteocyte: new insights, Annu. Rev. Physiol. 82 (2020) 485–506.
[9] L. Qin, W. Liu, H. Cao, G. Xiao, Molecular mechanosensors in osteocytes, Bone Res 8 (2020) 1–24.
[10] Y. Ishihara, Y. Sugawara, H. Kamioka, N. Kawanabe, H. Kurosaka, K. Naruse, T. Yamashiro, In situ imaging of the autonomous intracellular Ca^{2+} oscillations of osteoblasts and osteocytes in bone, Bone 50 (2012) 842–852.
[11] V.I. Sikavitsas, J.S. Temenoff, A.G. Mikos, Biomaterials and bone mechanotransduction, Biomaterials 22 (2001) 2581–2593.
[12] R. Ozasa, T. Ishimoto, S. Miyabe, J. Hashimoto, M. Hirao, H. Yoshikawa, T. Nakano, Osteoporosis changes collagen/apatite orientation and Young's modulus in vertebral cortical bone of rat, Calcif. Tissue Int. 104 (2019) 449–460.
[13] M. Tanaka, A. Matsugaki, T. Ishimoto, T. Nakano, Evaluation of crystallographic orientation of biological apatite at vertebral cortical bone in ovariectomized cynomolgus monkey treated with minodronic acid and alendronate, J. Bone Miner. Metabol. 34 (2016) 234–241.
[14] A. Matsugaki, N. Fujiwara, T. Nakano, Continuous cyclic stretch induces osteoblast alignment and formation of anisotropic collagen fiber matrix, Acta Biomater. 9 (2013) 7227–7235.
[15] A. Matsugaki, G. Aramoto, T. Nakano, The alignment of MC3T3-E1 osteoblasts on steps of slip traces introduced by dislocation motion, Biomaterials 33 (2012) 7327–7335.
[16] A. Matsugaki, Y. Isobe, T. Saku, T. Nakano, Quantitative regulation of bone-mimetic, oriented collagen/apatite matrix structure depends on the degree of osteoblast alignment on oriented collagen substrates, J. Biomed. Mater. Res. A. 103 (2015) 489–499.
[17] K.J. Lewis, D. Frikha-Benayed, J. Louie, S. Stephen, D.C. Spray, M.M. Thi, Z. Seref-Ferlengez, R.J. Majeska, S. Weinbaum, M.B. Schaffler, Osteocyte calcium signals encode strain magnitude and loading frequency in vivo, Proc. Natl. Acad. Sci. Unit. States Am. 114 (2017) 11775–11780.
[18] P.M. Govey, Y.I. Kawasawa, H.J. Donahue, Mapping the osteocytic cell response to fluid flow using RNA-Seq, J. Biomech. 48 (2015) 4327–4332.
[19] A.E. Morrell, G.N. Brown, S.T. Robinson, R.L. Sattler, A.D. Baik, G. Zhen, X. Cao, L. F. Bonewald, W. Jin, L.C. Kam, Mechanically induced Ca 2+ oscillations in osteocytes release extracellular vesicles and enhance bone formation, Bone Res 6 (2018) 1–11.
[20] T. Ganesh, L.E. Laughrey, M. Niroobakhsh, N. Lara-Castillo, Multiscale finite element modeling of mechanical strains and fluid flow in osteocyte lacunocanalicular system, Bone (2020) 115328.
[21] T. Adachi, Y. Aonuma, M. Tanaka, M. Hojo, T. Takano-Yamamoto, H. Kamioka, Calcium response in single osteocytes to locally applied mechanical stimulus: differences in cell process and cell body, J. Biomech. 42 (2009) 1989–1995.
[22] M. Oishi, S. Munesue, A. Harashima, M. Nakada, Y. Yamamoto, Y. Hayashi, Aquaporin 1 elicits cell motility and coordinates vascular bed formation by downregulating thrombospondin type-1 domain-containing 7A in glioblastoma, Cancer Med 9 (2020) 3904–3917.
[23] T. Shimasaki, S. Yamamoto, T. Arisawa, Exosome Research and Co-culture study, Biol. Pharm. Bull. 41 (2018) 1311–1321.
[24] Y. Li, S. Yuan, X. Wang, S.K. Tan, J. Mao, Comparison of flow fields in a centrifugal pump among different tracer particles by particle image velocimetry, ASME. J. Fluids Eng. 138 (2016), 061105.
[25] J. Jiang, R. Dingledine, Prostaglandin receptor EP2 in the crosshairs of anti-inflammation, anti-cancer, and neuroprotection, Trends Pharmacol. Sci. 34 (2013) 413–423.
[26] D. Shamir, S. Keila, M. Weinreb, A selective EP4 receptor antagonist abrogates the stimulation of osteoblast recruitment from bone marrow stromal cells by prostaglandin E2 in vivo and in vitro, Bone 34 (2004) 157–162.
[27] A.R. Stern, M.M. Stern1, M.E.V. Dyke, K. Jähn, M. Prideaux, L.F. Bonewald, Isolation and culture of primary osteocytes from the long bones of skeletally mature and aged mice, Biotechniques 52 (2012) 361–373.

[28] A. Matsugaki, D. Yamazaki, T. Nakano, Selective patterning of netrin-1 as a novel guiding cue for anisotropic dendrogenesis in osteocytes, Mater. Sci. Eng. C 108 (2020) 110391.
[29] Y. Kato, J.J. Windle, B.A. Koop, G.R. Mundy, L.F. Bonewald, Establishment of an osteocyte-like cell line, MLO-Y4, J. Bone Miner. Res. 12 (1997) 2014–2023.
[30] L.H. Xu, H. Shao, Y.-H.V. Ma, L. You, OCY454 osteocytes as an in vitro cell model for bone remodeling under mechanical loading, J. Orthop. Res. 37 (2019) 1681–1689.
[31] S.M. Woo, J. Rosser, V. Dusevich, I. Kalajzic, L.F. Bonewald, Cell line IDG-SW3 replicates osteoblast-to-late-osteocyte differentiation in vitro and accelerates bone formation in vivo, J. Bone Miner. Res. 26 (2011) 2634–2646.
[32] G. Nasello, P. Alamán-Díez, J. Schiavi, M. Pérez, L. McNamara, J.M. García-Aznar, Primary human osteoblasts cultured in a 3D microenvironment create a unique representative model of their differentiation into osteocytes, Front. Bioeng. Biotechnol. 8 (2020) 336.
[33] A. Matsugaki, T. Matuzaka, A. Murakami, P. Wang, T. Nakano, Three-dimensional printing of anisotropic bone mimetic structure with controlled fluid flow stimuli for osteocytes: flow orientation determines the elongation of dendrites, Int. J. Bioprint. 6 (2020) 293.
[34] J. Renaud, M.-G. Martinoli, Development of an insert co-culture system of two cellular types in the absence of cell-cell contact, JoVE J. Vis. Exp. (2016), e54356.
[35] L. Jia, W. Gu, Y. Zhang, Y. Ji, J. Liang, Y. Wen, X. Xu, The crosstalk between HDPSCs and HUCMSCs on proliferation and osteogenic genes expression in coculture system, Int. J. Med. Sci. 14 (2017) 1118–1129.
[36] C.D. Amo, V. Olivares, Matrix architecture plays a pivotal role in 3D osteoblast migration: the effect of interstitial fluid flow, J. Mech. Behav. Biomed. Mater. 83 (2018) 52–62.
[37] R. Ozasa, A. Matsugaki, T. Matsuzaka, T. Ishimoto, H.S. Yun, T. Nakano, Superior alignment of human iPSC-osteoblasts associated with focal adhesion formation stimulated by oriented collagen scaffold, Int. J. Mol. Sci. 22 (2021) 6232.
[38] X. Zhou, J.E. Novotny, L. Wang, Anatomic variations of the lacunar–canalicular system influence solute transport in bone, Bone 45 (2009) 704–710.
[39] C. Price, X. Zhou, W. Li, L. Wang, Real-time measurement of solute transport within the lacunar-canalicular system of mechanically loaded bone: direct evidence for load-induced fluid flow, J. Bone Miner. Res. 26 (2011) 277–285.
[40] A. Matsugaki, G. Aramoto, T. Ninomiya, H. Sawada, S. Hata, T. Nakano, Abnormal arrangement of a collagen/apatite extracellular matrix orthogonal to osteoblast alignment is constructed by a nanoscale periodic surface structure, Biomaterials 37 (2015) 134–143.
[41] S.W. Verbruggen, T.J. Vaughan, L.M. McNamara, Fluid flow in the osteocyte mechanical environment: a fluid–structure interaction approach, Biomech. Model. Mechanobiol. 13 (2014) 85–97.
[42] C.R. Jacobs, C.E. Yellowley, B.R. Davis, Z. Zhou, J.M. Cimbala, H.J. Donahue, Differential effect of steady versus oscillating flow on bone cells, J. Biomech. 31 (1998) 969–976.
[43] J. Li, E. Rose, D. Frances, Y. Sun, L. You, Effect of oscillating fluid flow stimulation on osteocyte mRNA expression, J. Biomech. 45 (2012) 247–251.
[44] M. Hu, G.-W. Tian, D.E. Gibbons, J. Jiao, Y.-X. Qin, Dynamic fluid flow induced mechanobiological modulation of in situ osteocyte calcium oscillations, Arch. Biochem. Biophys. 579 (2015) 55–61.
[45] S. Wang, S. Li, M. Hu, B. Huo, Calcium response in bone cells at different osteogenic stages under unidirectional or oscillatory flow, Biomicrofluidics 13 (2019), 064117.
[46] C. Wittkowske, G.C. Reilly, D. Lacroix, C.M. Perrault, In vitro bone cell models: impact of fluid shear stress on bone formation, Front. Bioeng. Biotechnol. 4 (2016) 87.
[47] I.P. Geoghegan, D.A. Hoey, L.M. McNamara, Estrogen deficiency impairs integrin αvβ3-mediated mechanosensation by osteocytes and alters osteoclastogenic paracrine signalling, Sci. Rep. 9 (2019) 1–15.
[48] M.M. Thi, S.O. Suadicani, M.B. Schaffler, S. Weinbaum, D.C. Spray, Mechanosensory responses of osteocytes to physiological forces occur along processes and not cell body and require αVβ3 integrin, Proc. Natl. Acad. Sci. Unit. States Am. 110 (2013) 21012–21017.
[49] R.M. Delaine-Smith, A. Sittichokechaiwut, G.C. Reilly, Primary cilia respond to fluid shear stress and mediate flow-induced calcium deposition in osteoblasts, Faseb. J. 28 (2014) 430–439.
[50] C. Galli, G. Passeri, G.M. Macaluso, Osteocytes and WNT: the mechanical control of bone formation, J. Dent. Res. 89 (2010) 331–343.
[51] D.A. Hoey, S. Tormey, S. Ramcharan, F.J. O'Brien, C.R. Jacobs, Primary cilia mediated mechanotransduction in human mesenchymal stem cells, Stem Cell. 30 (2012) 2561–2570.
[52] A.G. Robling, et al., Mechanical stimulation of bone in vivo reduces osteocyte expression of Sost/sclerostin, J. Biol. Chem. 283 (2008) 5866–5875.
[53] M.A. Kamel, J.L. Picconi, N. Lara-Castillo, M.L. Johnson, Activation of β-catenin si3naling in MLO-Y4 osteocytic cells versus 2T3 osteoblastic cells by fluid flow shear stress and PGE2: implications for the study of mechanosensation in bone, Bone 47 (2010) 872–881.
[54] M.R. Forwood, Inducible cyclo-oxygenase (COX-2) mediates the induction of bone formation by mechanical loading in vivo, J. Bone Miner. Res. 11 (1996) 1688–1693.
[55] P.P. Cherian, A.J. Siller-Jackson, S. Gu, X. Wang, L.F. Bonewald, E. Sprague, J. X. Jiang, Mechanical strain opens connexin 43 hemichannels in osteocytes: a novel mechanism for the release of prostaglandin, Mol. Biol. Cell 16 (2005) 3100–3106.
[56] Y. Boie, R. Stocco, N. Sawyer, D.M. Slipetz, M.D. Ungrin, F. Neuschäfer-Rube, G. P. Püschel, K.M. Metters, M. Abramovitz, Molecular cloning and characterization of the four rat prostaglandin E2 prostanoid receptor subtypes, Eur. J. Pharmacol. 340 (1997) 227–241.
[57] R. Mizuno, K. Kawada, Y. Sakai, Prostaglandin E2/EP signaling in the tumor microenvironment of colorectal cancer, Int. J. Mol. Sci. 20 (2019) 6254.
[58] S. Graham, Z. Gamie, I. Polyzois, A.A. Narvani, K. Tzafetta, E. Tsiridis, M. Heliotis, A. Mantalaris, E. Tsiridis, Prostaglandin EP2 and EP4 receptor agonists in bone formation and bone healing: in vivo and in vitro evidence, Expet Opin. Invest. Drugs 18 (2009) 749–766.
[59] D. Shamir, S. Keila, M. Weinreb, A selective EP4 receptor antagonist abrogates the stimulation of osteoblast recruitment from bone marrow stromal cells by prostaglandin E2 in vivo and in vitro, Bone 34 (2004) 157–162.
[60] K. Müller-Decker, C. Leder, M. Neumann, G. Neufang, F. Marks, G. Fürstenberger, C. Bayerl, J. Schweizer, Expression of cyclooxygenase isozymes during morphogenesis and cycling of pelage hair follicles in mouse skin: precocious onset of the first catagen phase and alopecia upon cyclooxygenase-2 overexpression, J. Invest. Dermatol. 121 (2003) 661–668.
[61] J.J. Egan, G. Gronowicz, G.A. Rodan, Cell density-dependent decrease in cytoskeletal actin and myosin in cultured osteoblastic cells: correlation with cyclic AMP changes, J. Cell. Biochem. 45 (1991) 93–100.
[62] C.H. Tang, R.S. Yang, W.M. Fu, Prostaglandin E2 stimulates fibronectin expression through EP1 receptor, phospholipase C, protein kinase C alpha, and c-Src pathway in primary cultured rat osteoblasts, J. Biol. Chem. 280 (2005) 22907–22916.
[63] A.V. Taubenberger, M.A. Woodruff, H. Bai, D.J. Muller, D.W. Hutmacher, The effect of unlocking RGD-motifs in collagen I on pre-osteoblast adhesion and differentiation, Biomaterials 31 (2010) 2827–2835.
[64] A. Matsugaki, S. Matsumoto, T. Nakano, A novel role of interleukin-6 as a regulatory factor of inflammation-associated deterioration in osteoblast arrangement, Int. J. Mol. Sci. 21 (2020) 6659.